



HHS Public Access

Author manuscript

Integr Biol (Camb). Author manuscript; available in PMC 2016 June 02.

Published in final edited form as:

Integr Biol (Camb). 2012 November ; 4(11): 1358–1366. doi:10.1039/c2ib20172k.

Imaging interactions of metal oxide nanoparticles with macrophage cells by ultra-high resolution scanning electron microscopy techniques†

Germán Plascencia-Villa^a, Clarise R. Starr^b, Linda S. Armstrong^b, Arturo Ponce^a, and Miguel José-Yacamán^a

Miguel José-Yacamán: miguel.yacaman@utsa.edu

^aDepartment of Physics and Astronomy, The University of Texas at San Antonio, One UTSA Circle, San Antonio, TX 78249, USA

^bU.S. Air Force School of Aerospace Medicine, Force Health Protection Technology and Global Health Surveillance (USAFSAM/FHT), 2510 Fifth Street, Wright-Patterson AFB, OH, USA

Abstract

Use of engineered metal oxide nanoparticles in a plethora of biological applications and custom products has warned about some possible dose-dependent cytotoxic effects. Macrophages are key components of the innate immune system used to study possible toxic effects and internalization of different nanoparticulate materials. In this work, ultra-high resolution field emission scanning electron microscopy (FE-SEM) was used to offer new insights into the dynamical processes of interaction of nanomaterials with macrophage cells dosed with different concentrations of metal oxide nanoparticles (CeO₂, TiO₂ and ZnO). The versatility of FE-SEM has allowed obtaining a detailed characterization of processes of adsorption and endocytosis of nanoparticles, by using advanced analytical and imaging techniques on complete unstained uncoated cells, including secondary electron imaging, high-sensitive backscattered electron imaging, X-ray microanalysis and stereoisimaging. Low voltage BF/DF-STEM confirmed nanoparticle adsorption and internalization into endosomes of CeO₂ and TiO₂, whereas ZnO develop apoptosis after 24 h of interaction caused by dissolution and invasion of cell nucleus. Ultra-high resolution scanning electron microscopy techniques provided new insights into interactions of inorganic nanoparticles with macrophage cells with high spatial resolution.

Introduction

The capacity to control size, shape and surface chemistry of engineered nanoparticles has enabled their use in a plethora of biological and medical applications, as drug delivery systems, therapeutics, diagnostics and imaging contrast agents with different advanced functions and new properties.^{1,2} Particularly, metal oxide nanoparticles are widely used in formulations of cosmetics, sunscreens, self-cleaning coatings and textiles, odor elimination products and for environment restoration-decontamination.³ Nevertheless, there are some

†Electronic supplementary information (ESI) available.

Correspondence to: Miguel José-Yacamán, miguel.yacaman@utsa.edu.

concerns about some potential dose-dependent toxicological and environmental effects after long-term exposition that could limit its usage.¹⁻⁵ Depending on particular nanoparticle properties and mechanisms of interaction with biological systems, adsorption and uptake can produce dose-dependent decrease in cell viability, also different metabolic and genetic alterations. These phenomena can be monitored with different well-established biochemical and molecular biology assays. In addition, microscopy methods are used to confirm attachment, internalization and intracellular localization of these nanomaterials.

Studies of detection and bio-distribution of nanoparticles with *in vitro* cell culture and tissues of animal models usually are studied by transmission electron microscopy (TEM), using resin embedded and heavy metal stained thin sections of cells. TEM alone cannot conclusively identify nanoparticles based on morphology due to particle aggregation, dissolution, contamination or morphology changes that could occur after cellular uptake.^{2,6} Besides that, traditional approaches are intricate, time-consuming and give partial two-dimensional images. Development of alternative and analytical methods to study interactions of nanoparticles with cells, to identify or discriminate possible toxic effects is imperative. For example, some theoretical methods based on physicochemical parameters can predict potential cytotoxic effects of metal oxide nanoparticles commonly used.³ Alternatives to image whole cells with electron microscopy involve use of special capsules and holders, and usually require sophisticated specimen preparation techniques.⁷⁻⁹

Field emission scanning electron microscopy (FE-SEM) coupled with energy dispersive X-ray (EDX) microanalysis and backscattered electron imaging (BEI) is an analytical technique used for identification and quantification of the precise elemental composition of a specimen.^{6,10} Ultra-high resolution SEM with cold field-emission guns, operated at low-voltages, has allowed novel applications and experimental approaches for life sciences, obtaining topographical information and detailed contrast of cellular features without the use of coating or heavy-metal staining, by coupling with specific analytical detectors and techniques to prepare biological samples.^{2,11,12} FE-SEM technologies continue to improve to provide insights into interactions at the nano-bio interface, with nanometer-scale resolution of surface morphology that previously could only be achieved with high voltage TEM. Backscattered electron detectors (LABE, Low-angle back-scattered electron; YAG-BSE, Yttrium-Aluminum-Garnet backscattered electron) provide qualitative compositional information of the sample, due to the production of back-scattered electrons being proportional to atomic number of the compounds and volume of the specimen. BEI are actually qualitative compositional maps obtained at deeper depths of the sample with a high spatial resolution. This imaging mode can be employed to confirm adsorption, uptake and intra-cellular location of nanoparticles in complete cells. Development of latest generation FE-SEM produces ultra-high resolution imaging, combined with precise quantitative measurements obtained by X-ray microanalysis.¹³

In this paper, assessment of biocompatibility and analysis of biological responses to nanoparticulate materials were studied with macrophages dosed with metal oxide nanoparticles. Ultra-high resolution advanced FE-SEM techniques revealed the interaction and precise details of adsorption, internalization and ultrastructural location of nanoparticles by key components of the innate immune system. The information obtained through advance

microscopy techniques is important for understanding the possible mechanisms involved in nanoparticle adsorption-uptake and to correlate with some potential cytotoxic effects.

Materials and methods

Characterization of metal oxide nanoparticles

Metal oxide nanoparticles (CeO₂, TiO₂ and ZnO) were obtained from NanoScale Corporation (Manhattan, KS, USA). Particles were diluted at 100 ppm, 20 µl drop of each sample was loaded on 300 mesh carbon/formvar copper grids (2SPI, West Chester, PA, USA) and dried before electron microscopy imaging. SEM imaging of metal oxide particles was performed with a HITACHI S-5500 FE-SEM. HR-TEM imaging was obtained with JEOL 2010-F at 200 kV (Peabody, MA, USA). Particles were diluted at 100–200 ppm in culture media to perform dynamic light scattering analysis. DelsaNano C (BeckmanCoulter, Brea, CA, USA) was used to obtain size distribution of particles by intensity and volume, and determine zeta potential of metal oxide nanoparticles in solution.

In vitro exposure of cells to metal oxide particles

Mouse macrophages J774A.1 cells (ATCC# TIB-67) were cultured in complete DMEM media (GIBCO, Carlsbad, CA, USA) supplemented with 10% FBS, NEAA, glutamine and 1% penicillin–streptomycin in an atmosphere of 100% humidity and 5% CO₂ at 37 °C. The cells were maintained in T-25 flasks to achieve 70–80% confluency before dosing of particles. Metal oxide particles were weighted in a dry powder and suspended in complete DMEM media as stock solutions at 10, 5, 1 and 0.1 mg ml⁻¹, vortex dispersed for 1 min and added to T-flasks to achieve final concentrations of 1, 0.5, 0.1 and 0.01 mg ml⁻¹, respectively. After 3 h incubation at 37 °C exhausted media were rinsed and attached cells were washed twice with PBS, cells were scraped and resuspended in 3 ml of PBS. Cell viability was evaluated by the Trypan blue exclusion method. Cells were centrifuged for 10 min at 1000 rpm at room temperature to form a pellet, PBS was rinsed and 1 ml of fixative buffer (phosphate buffered 4% formaldehyde, 1% glutaraldehyde, pH 7.2) was added to each sample. After 2 h incubation at room temperature cell pellets were stored at 4 °C.

FE-SEM imaging and X-ray microanalysis

Cells were loaded onto a 5 mm² silicon wafer, after 15 min incubation at room temperature excess buffer was removed with filter paper and stored in a desiccation chamber under vacuum.

SEM of complete cells was carried out with a S-5500 In-Lens FE-SEM (HITACHI, Tarrytown, NY, USA) coupled with LABE (Low Angle Backscattered Electron), YAG-BSE (Yttrium-Aluminum-Garnet Backscattered Electron), and solid state EDX detector (Bruker, Madison, WI, USA) operated with an accelerating voltage of 5–30 kV. Stereoimaging with SE and BEI detector modes of complete cells was obtained by collecting eucentric tilted high quality micrographs from –40° to +40°, illumination, contrast, magnification, working distance and tilting angle were determined to obtain 3D reconstruction and for further analysis.

Ultrastructural localization of particles

Fixed cell pellets were rinsed with PBS for 15 min and post-fixed with 1% OsO₄ in PBS for 1 h at room temperature. Samples were rinsed two times with PBS and dehydrated for 15 min with 25, 50, 75, 95 and 100% ethanol solutions, respectively. After two washes in propylene oxide, cell pellets were infiltrated with 50% LX112 resin (Ladd Research) in propylene oxide for 1 h. Finally, samples were infiltrated with 100% LX112 resin and cured at 60 °C for 48 h. Ultrathin sections (90 nm) were cut with Leica Ultracut ultramicrotome with a 45° diamond knife and mounted on 300 mesh copper grids (2PSI). Mounted sections were post-stained with 1% uranyl acetate solution for 30 min to increase contrast. Cell sections were imaged with BF/DF-STEM mode operated with an accelerating voltage of 5–30 kV.

Results and discussion

Characterization of metal oxide nanoparticles

Detailed and systematic characterization of nanomaterials is required as prerequisite for nanotoxicological studies, and to gain better understanding of influence of nanoparticle properties in the interaction with biological systems. Three metal oxides nanoparticles were selected: CeO₂, TiO₂ and ZnO, to assess interactions with macrophage cells through advanced electron microscopy applications. These nanoparticles were characterized by FE-SEM and HRTEM, observing a granulate morphology caused by tendency of nanoparticles to form aggregates, ranging from 50 to more than 500 nm for all particles analyzed (first column of Fig. 1). The specific sizes of primary particles that form these aggregates were determined by HRTEM (JEOL 2010F at 200 kV). Cerium and titanium oxide are formed by nanoparticles with diameter of 5–7 nm, whereas ZnO is formed by discrete crystalline particles of 5–10 nm (Fig. 1) (Table 1). Fast Fourier Transform (FFT) obtained from HRTEM images revealed interplanar spacing of 3.5 Å of fcc CeO₂ particle oriented in the $\langle 011 \rangle$ zone axis, 2.4 Å in the case of $\langle 111 \rangle$ oriented TiO₂ and 2.9 Å of ZnO nanoparticle oriented in the $\langle 111 \rangle$ zone axis. Crystallographic structure and chemical composition of nanoparticles were confirmed with XRD spectroscopy. Photon correlation spectroscopy (dynamic light scattering) was used to analyze size distribution and colloidal stability (zeta potential) of the particles in solution. Mean hydrodynamic diameter of nanoparticle aggregates in solution was of 277, 221 and 86 nm for CeO₂, TiO₂ and ZnO, respectively. In comparison, the particle size distribution of aggregates observed by electron microscopy changes drastically to 75, 42 and 68 nm for CeO₂, TiO₂ and ZnO (Table 1), this phenomenon has been attributed to dissolution and interaction with biomolecules of culture media.¹⁵ This tendency to form aggregates was confirmed by measurement of zeta potential, values obtained were of –4.83 mV (Cerium), 10.11 mV (Titanium) and 8.65 mV (Zinc), indicating an incipient colloidal instability of nanoparticles in solution that could cause sedimentation of nanoparticles.¹⁶

Imaging *in vitro* interaction of macrophages with metal oxide nanoparticles

Control macrophage cells prepared by the conventional method of fixation and dehydration^{11, 12} were mounted on cleaned silicon wafers. Cells appeared round shaped with high degree of spreading and around 10 µm in diameter (Fig. 2). Some cells appeared

flattened and with branched cytoplasm, and in some cases showing microvilli and small protrusions on the cell surface area.¹⁸ Ultra-high resolution FE-SEM imaging of complete cells was obtained without carbon or metal coating, or heavy-metal negative staining (osmium tetroxide), that are commonly used during preparation of biological samples. This minimal processing avoided possible charging effects and eventually damaging the cells, but also mainly any possible interference during X-ray microanalysis of cells dosed with metal oxide nanoparticles. Of the different acceleration voltages tested, 30 kV provided highest resolution images of complete cells (Fig. 2).

Assessment of biocompatibility and test of some possible cytotoxic effects of particulate materials is a standard practice.¹⁷ It involves *in vitro* interaction of cultured mammalian cells and nanomaterial tested under controlled and standardized conditions, and subsequent analysis of different biological responses to understand the interactions. Particularly, macrophages play a major role in innate immunity by recognition of antigens, internalization and processing of particulate targets, generally through process of phagocytosis.¹⁸⁻²⁰ FE-SEM imaging of complete unstained uncoated cells was used to reveal in high detail the processes of adsorption, and internalization of metal oxide nanoparticles by macrophages, also to examine bio-compatibility of nanomaterials tested. Fig. 3 and 4 show complete macrophages dosed with CeO₂ and TiO₂ nanoparticles, respectively. Panel A of both images reveals that metal oxide nanoparticles (white color aggregates) are attached to the cell membrane, and even some aggregates are already internalized through engulfing by endosomes. In comparison with control cells (Fig. 2), macrophages dosed with nanoparticles displayed small protrusions on the cell membrane on sites of adsorption of nanoparticles. Use of ultra-flat silicon wafers during SEM imaging avoids negative charging effects, commonly observed with biological samples. Use of conductive surfaces helps to improve quality of images obtained, especially with unstained and uncoated complete cells.²¹

The mechanisms of nanoparticle adsorption, uptake and biodistribution depend on size, shape, physicochemical and surface properties of nanomaterials, but also on specific cell type mechanisms.¹⁴ Our observations indicate that metal oxide nanoparticles seem to be internalized through endocytosis, the morphology of sites of adsorption corresponds to description of the endosome system.¹⁹ FE-SEM imaging revealed morphological details of complete dosed cells but with little compositional data. New generation of high sensitive solid-state annular backscattered electron detectors (LBE and YAG) eliminate some charge effects, providing rich qualitative compositional information through Z-contrast of nanoparticles, and internal structural information with a resolution similar or equivalent to SE detectors (5 nm).^{13,22} Biological materials have low electron scattering properties in comparison with metals, for that reason location of metal oxide nanoparticles is revealed as gray-black aggregates, with high contrast by an increased ratio of BSE to SE (Fig. 3B and 4B). Utility and versatility of backscattered electron imaging have been demonstrated with SEM imaging of location of Ag hybrid nanoparticles on U937 leukemia cells and Au nanoparticles on SK-BR-3 cancer cells.^{21,22} Identity and composition of nanoparticles was confirmed with EDX mapping, which generates a map of location of elements of interest (red dots, Fig. 3C and 4C), by scanning the sample surface to determine the concentration of particular elements at each point while imaging.^{6,10} The compositional image of EDX mapping with SE confirmed that aggregates observed with SE and LBE corresponded to

metal oxide nanoparticles that are attached to the cell membrane or already internalized by macrophages (Fig. 3D and 4D).

FE-SEM imaging of cells that were dosed with zinc oxide nanoparticles showed notorious changes in morphology of the cell membrane (Fig. 5), with the presence of large quantity of protrusions on sites of engulfing and adsorption of nanoparticles. Fig. 5B shows in detail the formation of invaginations of plasma membrane and formation of vesicles during the process of endocytosis. After adsorption, particles are rounded by structures formed on the cell membrane that engulf nanoparticles in a cytoplasmic phagosome; this process occurs by consecutive events of attachment and internalization of particles.¹⁹ Phagocytosis of particles occurs typically through receptor-mediated activation of F-actin-driven pseudopods that engulf and internalize the particles.^{18,23} Backscattered electron imaging showed that these endosomes are electrodense, indicating the presence of zinc oxide nanoparticles (Fig. 5C). EDX mapping of Zn confirmed identity and composition of nanoparticles in sites of adsorption/uptake (ESI[†]). The sample showed a background signal in all area scanned, this can be explained by the presence of Na in the fixative buffer used, and this compound has a peak with almost the same energy as Zn (1.012 keV). This could also be attributed to dissolution of ZnO nanoparticles into Zn²⁺ ions, as previously observed in *in vitro* studies.^{5,14}

Cell morphology can be studied using different imaging techniques, from classical optical microscopy to phase contrast, fluorescent, confocal, optical coherence tomography, and electron microscopy (SEM, FIB-SEM and TEM).²⁴⁻²⁶ Each method has particular advantages and limitations. We used stereoinaging SEM to reveal 3D cell morphology, to visualize and analyze in more detail the processes of adsorption and uptake of nanoparticles with nanometer-scale resolution. To obtain stereoinaging or pseudo-3D view of complete cells dosed with nanoparticles, we collected standardized eucentric tilted, high-quality SE and BEI images. Micrographs were recorded by varying orientation of complete uncoated cells from -40 to +40 degrees relative to the incident electron beam. Each image contains detailed information of cell morphology and location of metal oxide nanoparticles onto a single relative plane. Serial projections were combined in the superimposed reconstruction, obtaining stereoinage of complete cells using 3D reconstruction software (Image J). ESI[†] shows videos of reconstructed pseudo-3D view recorded with SE and LBE detectors of complete cells dosed with CeO₂ (video 1 and 2), TiO₂ (video 3 and 4) and ZnO (video 5 and 6).

This imaging technique can yield important information to visualize and analyze changes in 3D cell morphology, and details of cellular interactions with metal oxide nanoparticles tested, elucidating mechanisms of adsorption and uptake of nanomaterials on mammalian cells, and relating to dose-dependent cytotoxic effects observed. It was possible to observe some nanoparticle aggregates located inside rounded vesicles with high contrast with SE and LBE detectors, and track their location due to high Z-contrast of metal oxide nanoparticles. Besides cell morphology 3D reconstruction, BEI are actually qualitative compositional maps obtained at deeper depths in the sample with nearly the same spatial resolution as SE, confirming uptake and intracellular location of metal oxide nanoparticles in complete mammalian cells by FE-SEM applications. Stereoinaging is applied as a reliable analytic

method to reveal details of 3D cell morphology with nanometer scale resolution, to determine spatial distribution of nanoparticles throughout the cells or tissues, and in imaging of complex scaffold architectures and a diversity of bio- and nanomaterials.^{2,24}

Analysis of adsorption-uptake of metal oxide nanoparticles

Controversy related to potential cytotoxicity of nanoparticulate compounds persists. Especially oxide metals are used to achieve specific optical, electrical, and magnetic properties of functional materials. Biocompatibility, biodistribution and biodegradation of these nanomaterials need to be assessed to ensure their safety.¹⁴ Macrophage cells have been used extensively as an *in vitro* model of active antibody dependent phagocytosis, and to study possible toxic effects of different materials.¹⁹ We analyzed the dose-dependent effects of the metal oxide nanoparticles on cell viability by trypan blue exclusion. After 3 h of dosing, nanoparticles evaluated showed marked differences in profiles using the same doses and time of exposure (Fig. 6A). Adsorption and uptake of nanoparticles depend on different parameters, including size, shape, concentration, and superficial charge and coating, but if nanoparticles are not stable in colloidal suspension, they will sediment on cells.¹⁶ We observed that after 3 h of incubation the metal oxide nanoparticles sedimented on confluent cell monolayer; this phenomenon of incipient colloidal stability could increase the amount of interactions and uptake of nanoparticles by cells. Cerium oxide showed to be biocompatible in the concentration range of 50–500 ppm. Cells treated with CeO₂ maintained invariable viability even at high doses, and no evident signs of toxic effects were observed. In comparison, TiO₂ nanoparticles showed a clear dose-dependent reduction in number of viable cells, with no severe toxic effects on macrophages. With highest concentration probed, viability reached $66 \pm 1.25\%$ after 3 h of dosing with TiO₂. Measurements indicated that ZnO induced a drastic detriment in cell viability even at low doses, with maximum concentration used being 500 ppm and cell viability reached $60.9 \pm 8.1\%$ (Fig. 6A). As a consequence of ZnO treatment macrophages showed evident signs of cytotoxicity, as an increase in cell diameter and de-attachment of uniformly spread cell monolayer. Cytotoxic effects of ZnO have been observed in studies with human lung carcinoma cells and keratinocytes.^{5,27} Extended exposure time (24 h) confirmed that CeO₂ is biocompatible, cell viability on treatments with 100 ppm and 250 ppm were of $92 \pm 0.8\%$ and $87 \pm 0.6\%$, respectively. Previous studies have recognized that CeO₂ is biocompatible, and even biofunctional with antioxidant and anti-inflammatory properties.²⁸⁻³² Cells dosed with titanium oxide maintained cell viability of $93 \pm 1\%$ with 100 ppm, and with 250 ppm cell viability was recovered to $89.8 \pm 1.5\%$, in comparison with $77 \pm 0.7\%$ at 3 h of dosing (Fig. 6A). Finally, nanoparticulate ZnO showed a remarkable effect on cell viability, reaching $23.5 \pm 10.6\%$ and $21 \pm 4.3\%$, upon treatments with 100 and 250 ppm, respectively. We observed a complete detachment of cells from the culture surface and changes in cell morphology. Cytotoxic effects of ZnO occur through rapid dissolution of nanoparticles, releasing toxic Zn²⁺ cations in culture media in a short period of time (<3 h), developing oxidative stress, lysosomal damage and inflammation.^{15,30} Interaction of metal oxide nanoparticles on cells may lead to a cascade of biological responses. Cytotoxic effects and acute dose-dependent decrease in cell viability by metal oxides in the nanometer range are related to different mechanisms, including production of reactive oxygen species (ROS) and cytokines, oxidative stress, dissolution and release of cationic ions, inflammation, protein

aggregation, deregulation of gene expression, and alterations in cell membrane functions.^{2,3,15,30} Several studies indicate that free ions released from nanoparticles can cause oxidative stress in high doses, even at short periods of time of exposition, by exceeding metabolic capabilities to deal with metal ions.^{14,15,30}

In order to determine whether the cytotoxic effects observed correlate with the amount of adsorbed nanomaterial to cells, the quantity of nanoparticles was measured by X-ray microanalysis. Mechanisms for recognition and uptake of nanoparticles by biological systems are related to cell receptors, and structural properties of nanoparticles (size, shape, charge and functionalization). Particularly, particles with diameter below 100 nm are efficiently internalized by cells.^{1,18,19} Fig. 6B, shows profiles of particles quantified (expressed as wt%) on cells treated at different concentrations probed, and obtained from integration of characteristic peaks of corresponding EDX spectra. X-ray microanalysis was used as a standardized technique as it is capable of detecting and quantifying elemental composition in an unbiased manner, reducing ambiguities in nanoparticle aggregation, contamination, or changes in morphology after cell adsorption and uptake.^{6,10,17,33} Fig. 6C shows typical X-ray spectra obtained from cells dosed with metal oxide nanoparticles. EDX peaks of C, N, O and metal (Ce, Ti or Zn) were integrated to calculate wt% of particles adsorbed on cells. Characteristics peaks of Ce are located at 0.883 and 4.839 keV, 0.452 and 4.510 for Ti peaks, and in the case of Zn, 1.012 and 8.637 keV; all of them are clearly distinguishable.

Ultrastructural location of metal oxide nanoparticles

Studies of detection and bio-distribution of nanoparticles in cells and tissues usually employ transmission electron microscopy (TEM). We employed high-resolution low voltage STEM imaging with a BF/DF Duo-STEM detector to obtain high-contrast electron micrographs of thin sections of cells, and EDX mapping to confirm chemical composition. Low voltage STEM is a new field of high-resolution electron microscopy that uses low electron doses (1–30 kV) but with notable finite spatial resolution (1.6 nm @ 1 kV, 0.4 nm @ 30 kV), minimizing radiation damage of sensitive samples for high-resolution imaging and EDX microanalysis. Additionally, BEI can be applied on resin embedded biological samples under low accelerating voltage and low beam current conditions, to drastically enhance compositional contrast and resolution to analyze cell organelles and subcellular structures.²⁵

Macrophages dosed with 250 ppm of metal oxide nanoparticles for 3 h were processed to assess ultrastructural localization of nanoparticles. Fig. 7 revealed that cells avidly phagocytised large aggregates of cerium oxide within 3 h of dosing. Particles seemed to be attached to the cell membrane and some aggregates located into membrane protuberances forming phagosomes. Dark field (DF-STEM) imaging, providing atomic number (Z contrast) was used to locate areas of location of metal oxide nanoparticles for EDX microanalysis. Fig. 7A and B shows details of cerium nanoparticles during the process of endocytosis, and the formation of protuberances in the cell membrane to engulf the aggregates. YAG-BSE imaging confirmed location of CeO₂ nanoparticle aggregates with a strong contrast due to Z differences, confirming the elemental analysis of the sample. It was possible to distinguish some organelles as nucleus, mitochondria, endoplasmic reticulum,

and especially nuclear membrane even at this low voltage used (5–30 kV). Chemical composition of the sample was confirmed with energy dispersive X-ray (EDX) analysis, revealing distribution of NP attached to the cell membrane and intracellularly (ESI[†]). Toxicity of CeO₂ nanoparticles to mammalian cells has been analyzed in previous studies, after uptake particles were localized into endosomes of mouse monocyte/macrophages and human epithelial cells; this process occurred without cytotoxic effects or inflammation.¹⁵ Cerium oxide particles have been proposed to be a therapeutical antioxidant agent, by conferring cellular protection *in vitro* and *in vivo*, also increasing cell surveillance mainly by suppression of reactive oxygen species (ROS) that could cause oxidative stress.^{21,24,25,34}

Fig. 7C shows that titanium oxide nanoparticles are located intracellularly into big aggregates, surrounded by membranes that correspond to endosomes. These observations correlate with FE-SEM imaging of complete cells that revealed attachment and uptake of TiO₂ by macrophages. It is clear the presence of membrane surrounded the nanoparticle aggregates internalized through the process of phagocytosis (Fig. 7D).^{18,35,36} BEI showed location of high contrast aggregates corresponding to Ti nanoparticles, whereas EDX mapping confirmed chemical composition and relative concentration of Ti of electrodeposited aggregates by mapping of Ti-KA and the presence of characteristic peaks of Ti in EDX spectra (ESI[†]). Evaluation of toxicity of TiO₂ revealed that it is the least toxic nanomaterial accumulated into lysosomes, but with no cellular protective effects. Only at high concentrations (over 100 mg m⁻¹) TiO₂ particles developed cytotoxic effects in fibroblasts and lung epithelial cells.^{15,28}

FE-SEM of complete cells dosed with zinc oxide nanoparticles showed that this compound appears as aggregates located in phagosomes. Thin sections of cells doped with ZnO showed that the inorganic compound appeared located intra-cytoplasmically and into nucleus, but not inside specific structures like lysosomes, in contrast with cerium and titanium oxide nanoparticles mainly located attached to the cell membrane or into lysosomes. Identification of ZnO nanoparticles, remains ambiguous due to possible morphology change (by changes in pH during the process of internalization), aggregation and dissolution into Zn²⁺ ions.⁶ BEI and EDX mapping of Zn confirm chemical composition of the sample and give information about the relative distribution of Zn-L (ESI[†]). The Zn signal was detected over the entire surface area, but with high concentration in electrodeposited regions observed by low voltage STEM. Treatments with ZnO at 3 h caused changes in structure, compromising cell membrane integrity, blebbing and formation of apoptotic bodies. Particle invasion into the cell nucleus was evident, causing characteristic mechanisms of condensation of DNA. Similar observations of dose-dependent toxic effects and induction of cell death through apoptosis by ZnO particles have been observed in different cell models, including monocyte-derived macrophages, epithelial cells, mouse neural stem cells, human brain tumor U87, HeLa and HEK cells.^{15,18,35,38}

Macrophages were incubated for 24 h to analyze the effect after longer time of exposition, degradation and ultra-structural location of metal oxide nanoparticles. Interaction of cells with nanomaterials can include cellular uptake, membrane perturbations, transcytosis, intracellular transport and processing, that in some cases derive in cell necrosis or apoptosis.²³ Cells treated with CeO₂ and TiO₂ showed that the nanoparticle aggregates

suffered dissolution and particle invasion into the cell nucleus was observed in both cases (Fig. 8). No signs of necrosis, apoptosis or chromatic condensation were observed; organelles and cell membrane showed similar morphology to cells treated for only 3 h. In comparison, after 24 h exposure to ZnO, macrophages showed advanced signs of apoptosis, including nucleus, cell membrane and organelles severely compromised with evident damage and cracked (Fig. 8E and F). Nanoparticle aggregates were no longer distinguishable, EDX mapping indicate that ZnO suffered dissolution and dispersed through sample.

Conclusions

Detailed information on interactions of cells with nanostructured materials commonly used in consumer products is required, to fully exploit the tremendous potential of emerging rapidly developing area of nanotechnology. We showed ultra high-resolution FE-SEM analytical studies as an approach to assess and compare interactions of metal oxide nanoparticles with mammalian cells.

Information obtained was used to interpret biological responses and to determine some correlations with physicochemical and structural properties of nanoparticles used in *in vitro* assays. New generation of SE and BEI detectors allowed obtaining ultra high-resolution imaging of cell morphology, without use of any staining with heavy-metal ions or coating. Use of BEI and X-ray micro-analysis helped to confirm internalization and chemical composition of metal oxide nanoparticles on uncoated and unstained complete cells. Complementary high-contrast low voltage STEM of thin sections of dosed cells confirmed nanoparticle adsorption, uptake and ultra-structural location of metal oxide nanoparticles. This imaging mode allows simultaneous bright and dark field imaging at low voltage doses in thin section samples with high finite spatial resolution. In particular we observed signs of apoptosis caused by ZnO, dissolution of nanoparticle aggregates and invasion into the cell nucleus after 24 h of interaction. FE-SEM provides versatile applications to study interactions of nanoparticles with living organisms, especially to elucidate biocompatibility, biodistribution and biodegradation of nanoparticles with high spatial resolution, good depth of field and sub-nanometer resolution.

Supplementary Material

Refer to Web version on PubMed Central for supplementary material.

Acknowledgments

This work was supported by US Air Force grant (FA8650-10-2-6145), NIH-RCMI (G12MD007591), NSF-PREM (DMR-0934218), The Welch Foundation (AX-1615) and CONACyT (147947 and 173179). Technical support was provided by Jonathan Grossheim and Keegan Hanks. We acknowledge access to cell culture facilities of UTSA Department of Biology (Dr Andrew Tsin, Brandi Betts and Daniel I. Obregon) and USAFSAM/FHT (Elia Villazana); DLS of UTSA Department of Civil and Environmental Engineering (Dr Heather Shipley and Jinxuan Hu).

References

1. Albanese A, Sykes EA, Chan WC. ACS Nano. 2010; 4:2490–2493. [PubMed: 20496953]

2. Schrand AM, Schlager JJ, Dai L, Hussain SM. *Nat Protoc.* 2010; 5:744–757. [PubMed: 20360769]
3. Puzyn T, Rasulev B, Gajewicz A, Hu X, Dasari TP, Michalkova A, Hwang HM, Toropov A, Leszczynska D, Leszczynski J. *Nat Nanotechnol.* 2011; 6:175–178. [PubMed: 21317892]
4. Hoet PH, Nemmar A, Nemery B. *Nat Biotechnol.* 2004; 22:19. [PubMed: 14704693]
5. Horie M, Fujita K, Kato H, Endoh S, Nishio K, Komaba LK, Nakamura A, Miyauchi A, Kinugasa S, Hagihara Y, Niki E, Yoshida Y, Iwahashi H. *Metallomics.* 2012; 4:350–360. [PubMed: 22419205]
6. Zheng J, Nagashima K, Parmiter D, de la Cruz J, Patri AK. *Methods Mol Biol (N Y, NY, U S).* 2011; 697:93–99.
7. De Jonge N, Peckys DB, Kremers GJ, Piston DW. *Proc Natl Acad Sci U S A.* 2009; 106:2159–2164. [PubMed: 19164524]
8. Flannigan DJ, Barwick B, Zewail AH. *Proc Natl Acad Sci U S A.* 2010; 107:9933–9937. [PubMed: 20479261]
9. Peckys DB, Veith GM, Joy DC, de Jonge N. *PLoS One.* 2009; 4:e8214. [PubMed: 20020038]
10. Patri A, Umbreit T, Zheng J, Nagashima K, Goering P, Francke-Carroll S, Gordon E, Weaver J, Miller T, Sadrieh N, McNeil S, Stratmeyer M. *J Appl Toxicol.* 2009; 29:662–672. [PubMed: 19626582]
11. Schatten, H. *Biological low voltage scanning electron microscopy.* Schetten, H.; Pawle, J., editors. Springer; 2008. p. 145-169.
12. Schatten H. *Micron.* 2011; 42:175–185. [PubMed: 21036051]
13. Schwandt CS. *Am Lab.* 2010; 6:13–17.
14. Kunzmann A, Andersson B, Thurnherr T, Krug H, Scheynius A, Fadeel B. *Biochim Biophys Acta.* 2011; 1810:361–373. [PubMed: 20435096]
15. Xia T, Kovochich M, Liong M, Mädler L, Gilbert B, Shi H, Yeh JI, Zink JI, Nel AE. *ACS Nano.* 2008; 2:2121–2134. [PubMed: 19206459]
16. Cho EC, Zhang Q, Xia Y. *Nat Nanotechnol.* 2011; 6:385–391. [PubMed: 21516092]
17. ASTM Standard Test Method F 1903-98R03. www.astm.org
18. Krysko DV, Denecker G, Festjens N, Gabriels S, Parthoens E, D'Herde K, Vandenabeele P. *Cell Death Differ.* 2006; 13:2011–2022. [PubMed: 16628234]
19. Ralph P P, Nakoinz I. *Nature.* 1975; 257:393–394. [PubMed: 1101071]
20. Sharma V, Singh SK, Anderson D, Tobin DJ, Dhawan A, Nanosci J. *Nanotechnol.* 2011; 11:3782–3788.
21. Suh WH, Suslick KS, Stucky GD, Suh YH. *Prog Neurobiol (Oxford, U K).* 2009; 87:133–170.
22. Auffan M, Rose J, Bottero JY, Lowry GV, Jolivet JP, Wiesner MR. *Nat Nanotechnol.* 2009; 4:634–641. [PubMed: 19809453]
23. Nel AE, Mndler L, Velegol D, Xia T, Hoek EM, Somasundaran P, Klaessig F, Castranova V, Thompson M. *Nat Mater.* 2009; 8:543–557. [PubMed: 19525947]
24. Hirst SM, Karakoti AS, Tyler RD, Sriranganathan N, Seal S, Reilly CM. *Small.* 2009; 5:2848–2856. [PubMed: 19802857]
25. Karakoti AS, Monteiro-Riviere NA, Aggarwal R, Davis JP, Narayan RJ, Self WT, McGinnis J, Seal S. *J Mater Sci (1989).* 2008; 60:33–37.
26. Huotari J, Helenius A. *EMBO J.* 2011; 30:3481–3500. [PubMed: 21878991]
27. Chen HH, Chien CC, Petibois C, Wang CL, Chu YS, Lai SF, Hua TE, Chen YY, Cai X, Kempson IM, Hwu Y, Margaritondo G. *J Nanobiotechnol.* 2011; 9:14.
28. Koh AL, Shachaf CM, Elchuri S, Nolan GP, Sinclair R. *Ultramicroscopy.* 2008; 109:111–121.
29. Champion JA, Mitragotri S. *Proc Natl Acad Sci U S A.* 2006; 103:4930–4934. [PubMed: 16549762]
30. Jones CF, Grainger DW. *Adv Drug Delivery Rev.* 2009; 61:438–456.
31. Hartsuiker L, Van Es P, Petersen W, Van Leeuwen TG, Terstappen LW, Otto C. *J Microsc (Paris).* 2011; 244:187–193.
32. Cuijpers VM, Walboomers XF, Jansen JA. *Tissue Eng, Part C.* 2011; 17:663–668.

33. Ohta K, Sadayama S, Togo A, Higashi R, Tanoue R, Nakamura KI. *Micron*. 2012; 43:612–620. [PubMed: 22285616]
34. Smith LE, Smallwood R, Macneil S. *Microsc Res Tech*. 2010; 73:1123–1133. [PubMed: 20981758]
35. Singh S, Kumar A, Karakoti A, Seal S, Self WT. *Mol Biosyst*. 2010; 6:1813–1820. [PubMed: 20697616]
36. Müller KH, Kulkarni J, Motskin M, Goode A, Winship P, Skepper JN, Ryan MP, Porter AE. *ACS Nano*. 2010; 4:6767–6779. [PubMed: 20949917]
37. Deng X, Luan Q, Chen W, Wang Y, Wu M, Zhang H, Jiao Z. *Nanotechnology*. 2009; 20:115101. [PubMed: 19420431]
38. Zvyagin AV, Zhao X, Gierden A, Sanchez W, Ross JA, Roberts MS. *J Biomed Opt*. 2008; 13:064031. [PubMed: 19123677]

Insight, innovation, integration

This paper analyzes the interaction of macrophages with metal oxide nanoparticles through using ultra high-resolution FE-SEM analytical applications, to gain detailed visualization of the dynamic processes of adsorption and internalization of nanostructured materials. Use of advanced FE-SEM on unstained uncoated cells, coupled with high-sensitive back-scattered electron imaging, low voltage STEM and energy dispersive X-ray microanalysis. Use of versatile analytical tools to elucidate processes that occur during interaction of mammalian cells with nanostructured materials at high spatial resolution and low voltage doses. This paper shows how advanced scanning electron microscopy techniques provide valuable information to understand interactions of functionally engineered nanoparticles with immune cells and to correlate with some dose-dependent cytotoxic effects.

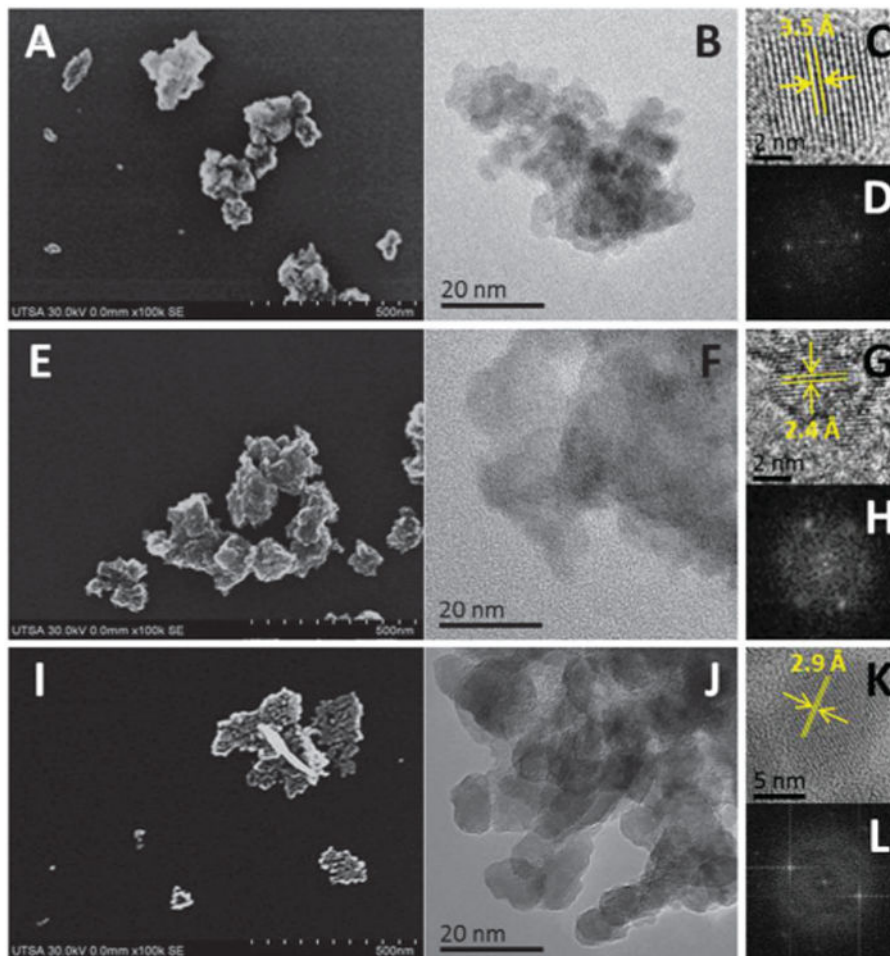


Fig. 1. Characterization of metal oxide nanoparticles. (A) FE-SEM of CeO_2 , (B) HR-TEM of CeO_2 , (C) CeO_2 nanoparticle, (D) FFT of (C), (E) FE-SEM of TiO_2 , (F) HR-TEM of TiO_2 , (G) TiO_2 nanoparticle, (H) FFT of (G), (I) FE-SEM of ZnO , (J) HR-TEM of ZnO , (K) ZnO nanoparticle, (L) FFT of (K).

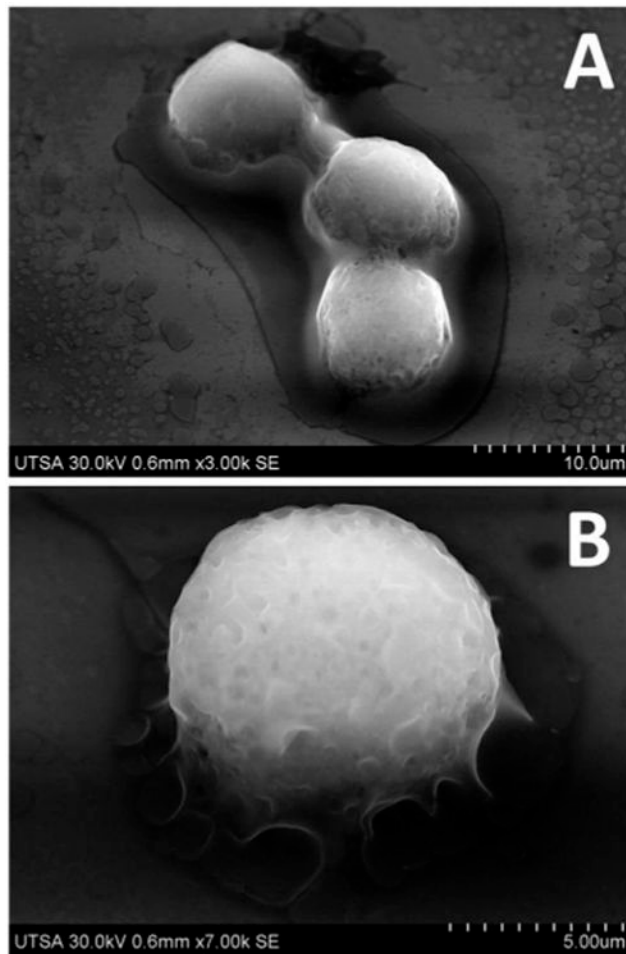


Fig. 2. FE-SEM imaging of complete cells. Fixed macrophage cells imaged at 30 kV (sample tilted -32°).

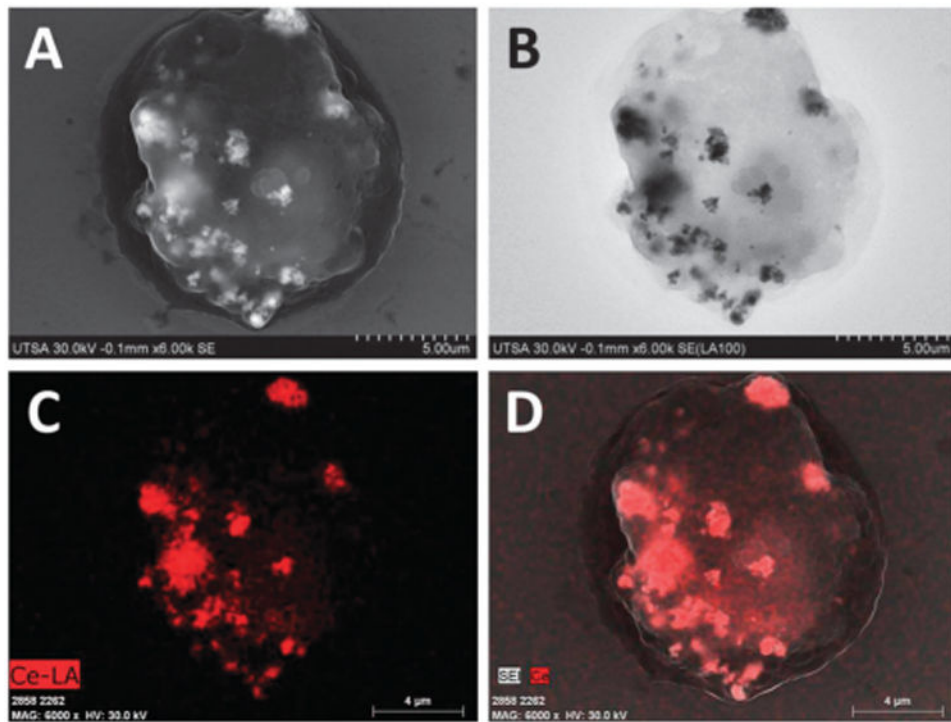


Fig. 3. FE-SEM imaging of complete cells dosed with CeO₂ nanoparticles. (A) SE imaging. (B) LBE Imaging. (C) EDX mapping of Ce-LA. (D) Merge.

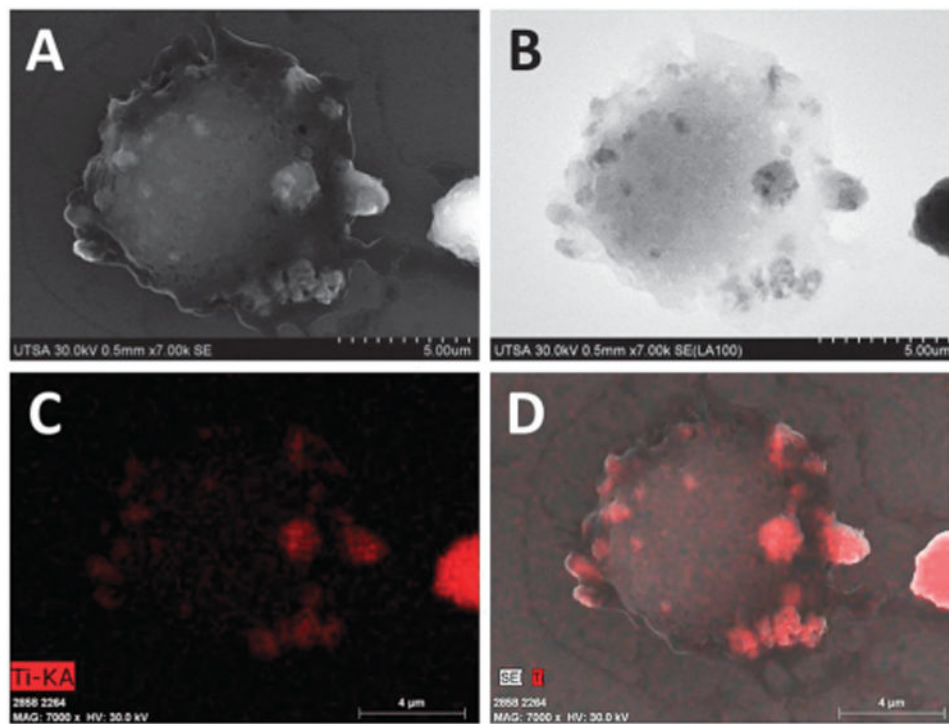


Fig. 4. FE-SEM imaging of complete cells dosed with TiO₂ nanoparticles. (A) SE imaging. (B) LBE Imaging. (C) EDX mapping of Ti-KA. (D) Merge.

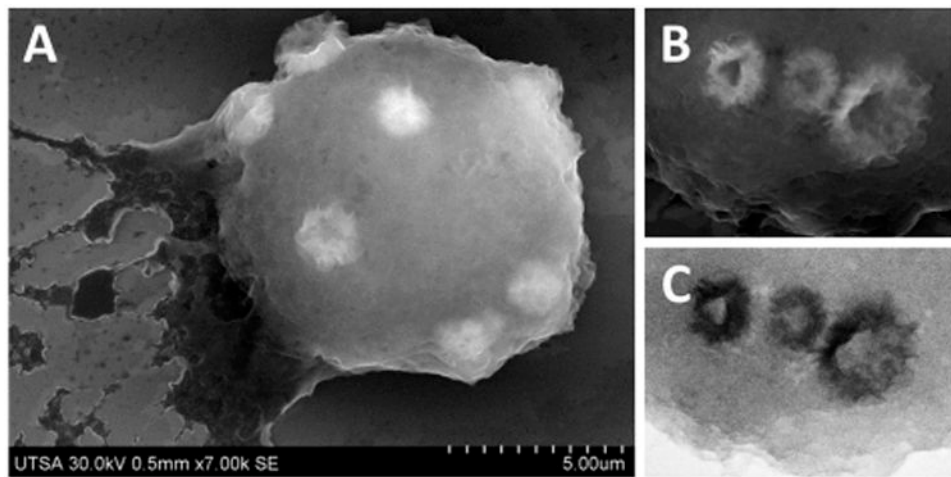


Fig. 5. FE-SEM imaging of complete cells dosed with ZnO nanoparticles. (A) SE imaging. (B) SE imaging detail of cell membrane. (C) LBE imaging detail of cell membrane.

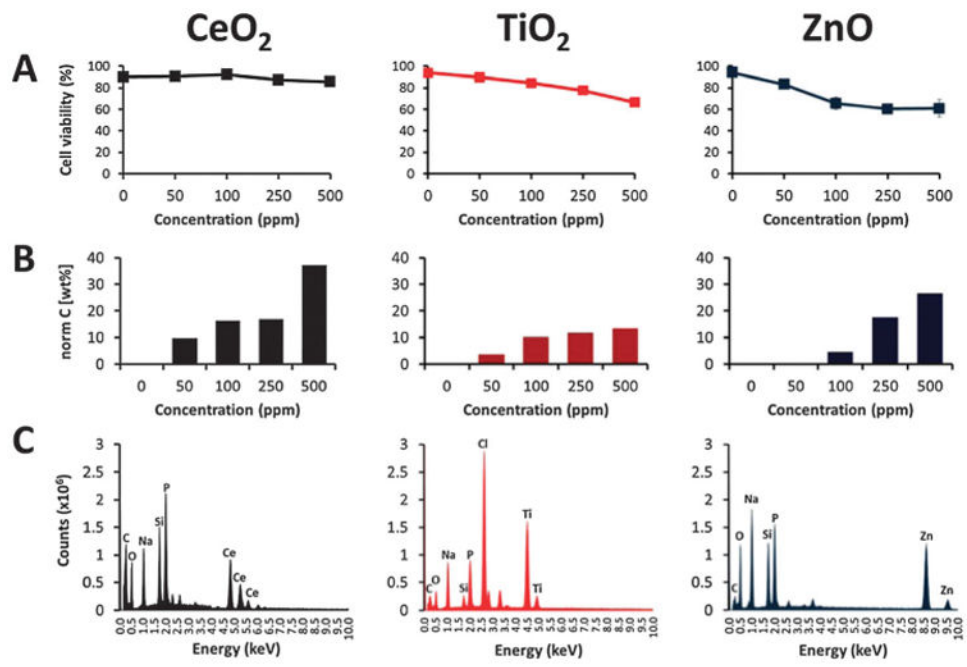


Fig. 6. Viability and X-ray microanalysis of cells dosed with metal oxide nanoparticles. (A) Cell viability. (B) Quantification by X-ray microanalysis. (C) X-ray spectra.

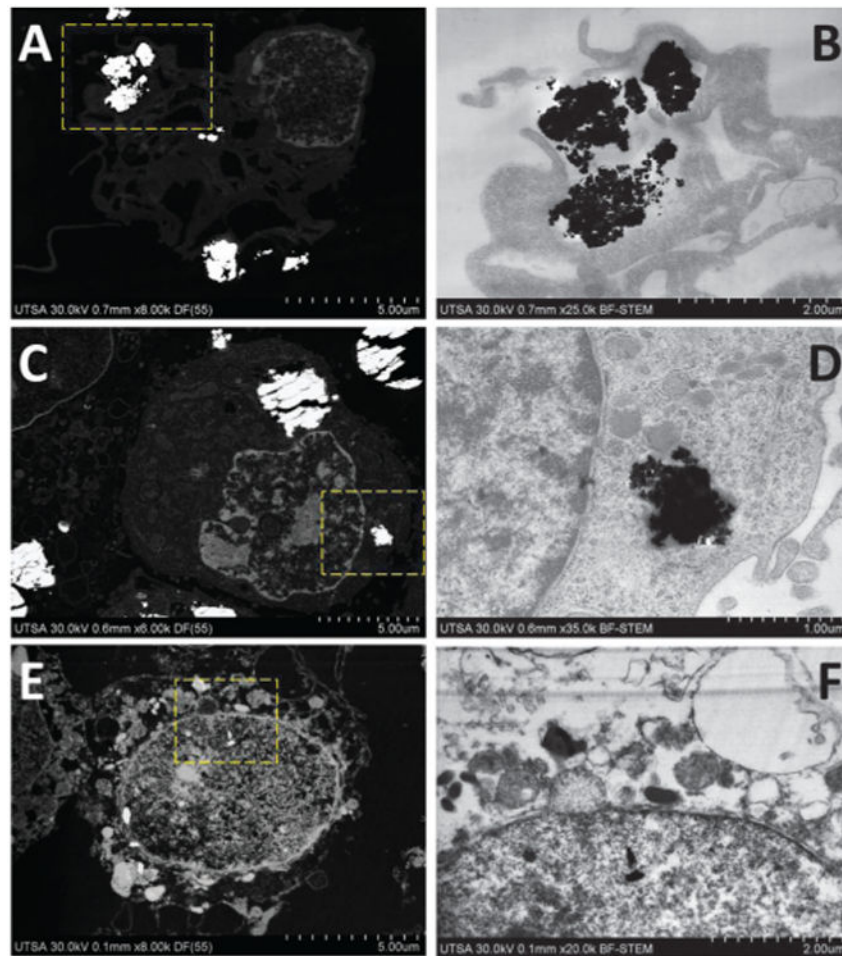


Fig. 7. Ultrastructural location of nanoparticles into macrophage cells after 3 h. (A) DF-STEM imaging of CeO₂. (B) BF-STEM imaging, selected area of (A). (C) DF-STEM imaging of TiO₂. (D) BF-STEM imaging, selected area of (C). (E) DF-STEM imaging of ZnO. (F) BF-STEM imaging, selected area of (E).

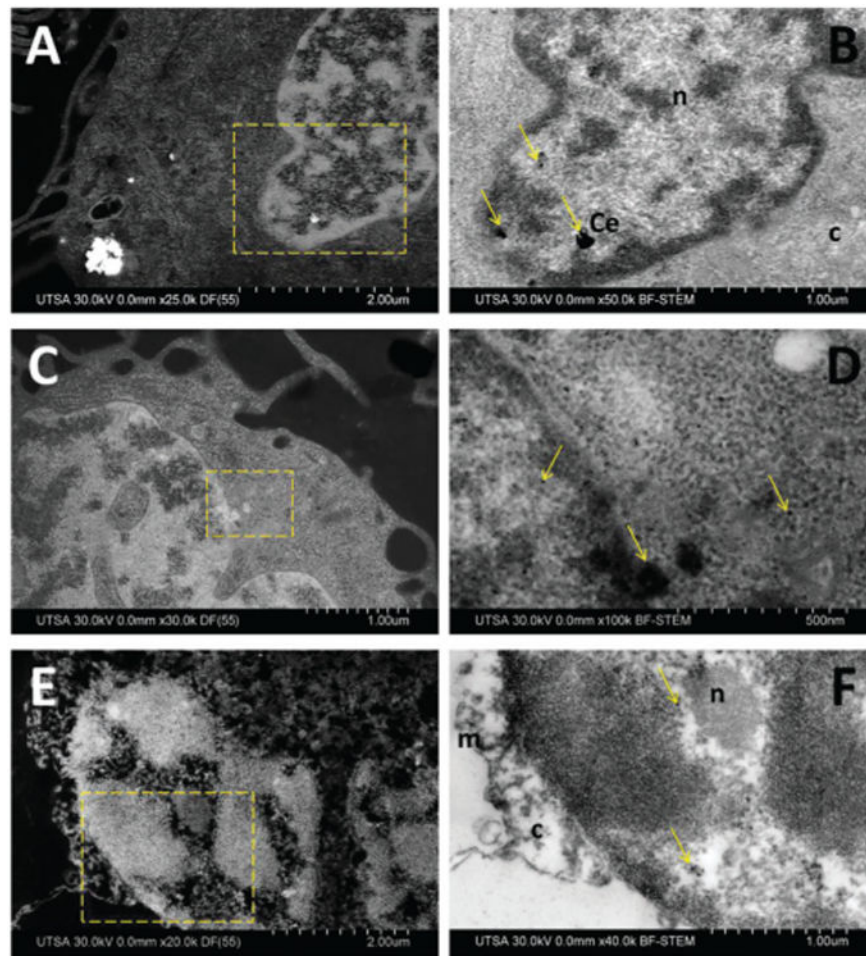


Fig. 8. Ultrastructural location of nanoparticles into macrophage cells after 24 h. (A) DF-STEM imaging of CeO_2 . (B) BF-STEM imaging, selected area of (A). (C) DF-STEM imaging of TiO_2 . (D) BF-STEM imaging, selected area of (C). (E) DF-STEM imaging of ZnO . (F) BF-STEM imaging, selected area of (E). Arrows indicate location of nanoparticles, n (nucleus), c (cytoplasm), m (membrane).

Table 1
Characterization of metal oxide nanoparticles

Nanoparticle	Single particle size (nm)	Particle aggregate size (nm)	Hydrodynamic diameter (nm)	Zeta potential (mV)
Cerium oxide	5–7	75	277	–4.83
Titanium oxide	5–7	42	271	+10.11
Zinc oxide	5–10	68	86	+8.65

Author Manuscript

Author Manuscript

Author Manuscript

Author Manuscript